Acta Crystallographica Section D
Biological Crystallography
ISSN 0907-4449

Further insights into the mechanism of function of the response regulator CheY from crystallographic studies of the CheY–CheA$_{124–257}$ complex

P. Gouet, N. Chinardet, M. Welch, V. Guillet, S. Cabantous, C. Birck, L. Mourey and J.-P. Samama*

Groupe de Cristallographie Biologique, IPBS-CNRS, 205 Route de Narbonne, 31077 Toulouse CEDEX, France

Correspondence e-mail: samama@ipbs.fr

Received 25 August 2000
Accepted 23 October 2000

PDB References: native CheY–CheA$_{124–257}$ complex, 1ffg; acetyl phosphate soaked CheY–CheA$_{124–257}$ complex, 1ffs; imido-diphosphate soaked CheY–CheA$_{124–257}$ complex, 1ffw.

New crystallographic structures of the response regulator CheY in association with CheA$_{124–257}$, its binding domain in the kinase CheA, have been determined. In all crystal forms, the molecular interactions at the heterodimer interface are identical. Soaking experiments have been performed on the crystals using acetyl phosphate as phosphodonor to CheY. No phosphoryl group attached to Asp57 of CheY is visible from the electron density, but the response regulator in the CheY–CheA$_{124–257}$ complex may have undergone a phosphorylation–dephosphorylation process. The distribution of water molecules and the geometry of the active site have changed and are now similar to those of isolated CheY. In a second soaking experiment, imido-diphosphate, an inhibitor of the phosphorylation reaction, was used. This compound binds in the vicinity of the active site, close to the N-terminal part of the first α-helix. Together, these results suggest that the binding of CheY to CheA$_{124–257}$ generates a geometry of the active site that favours phosphorylation and that imido-diphosphate interferes with phosphorylation by precluding structural changes in this region.

1. Introduction

Two-component systems are prevalent signalling phosphorelay cascades responsible for signal transduction in prokaryotes (Stock *et al.*, 1995; Goudreau & Stock, 1998) and are also found in some eukaryotes (Mizuno, 1998). One of these systems mediates bacterial chemotaxis and involves the well studied CheA and CheY proteins (Barak & Eisenbach, 1996). CheA is a class II histidine kinase (Dutta *et al.*, 1999) coupled to membrane receptors. Ligand binding to the periplasmic domain of these receptors controls the phosphorylation state of the kinase (Liu *et al.*, 1997; Grebe & Stock, 1999). The phosphoryl group is transfered in turn to the response regulator CheY, whose activated form binds to the protein FliM of the flagella motor (Bren & Eisenbach, 1998; McEvoy *et al.*, 1999). Phosphotransfer from the kinase to the response regulator is magnesium dependent in all two-component systems (Stock *et al.*, 1993).

CheA is composed of functional regions connected by flexible linkers (Oosawa *et al.*, 1988). The N-terminal domain (CheA$_{1–134}$) is termed P1 and carries the phosphorylatable histidine residue. The second domain (CheA$_{159–227}$) or P2 module provides the binding region for CheY. It contributes to the specificity of the phosphotransfer reaction and may enhance the rate of phosphotransfer (Li *et al.*, 1995; Swanson *et al.*, 1995). The folds of the P1 and P2 modules have been revealed by heteronuclear NMR spectroscopy (Zhou *et al.*, 1995; McEvoy *et al.*, 1996). P1 displays a four-helix bundle

motif and P2 appears as an open-face β/α sandwich consisting of four antiparallel β-strands and two α-helices. The third region of CheA is responsible for dimerization, catalytic activity and interactions with upstream proteins (Liu *et al.*, 1997; Levit *et al.*, 1998). These functions are carried out by dedicated domains as revealed by the X-ray structure (Bilwes *et al.*, 1999).

The response regulator CheY is an isolated receiver domain of molecular weight 14 kDa. It is phosphorylated on an aspartate residue, an invariant amino acid in the superfamily of response regulators. Several structures of CheY from various bacteria have been solved [*Salmonella typhimurium* (Stock *et al.*, 1989), *Escherichia coli* (Volz & Matsumura, 1991; Bellsolell *et al.*, 1994), *Thermatoga maritima* (Usher *et al.*, 1998)]. CheY displays the doubly wound $(\beta/\alpha)_5$ fold shared by all receiver domains in response regulators (Volkman *et al.*, 1995; Baikalov *et al.*, 1996; Madhusudan *et al.*, 1997; Gouet, Fabry *et al.*, 1999; Müller-Dieckmann *et al.*, 1999; Sola *et al.*, 1999).

The structure of CheY–CheA$_{124–257}$ (CheY–P2) from *E. coli* was the first report of a protein complex in the two-component systems (Welch *et al.*, 1998). It was crystallized in space group $P2_1$, with four molecules of the complex in the asymmetric unit. The structure was refined using data to 3 Å resolution with no water molecules included. The structure of the same complex obtained from a slightly different construct of CheA and under different crystallization conditions was then reported to 2 Å (McEvoy *et al.*, 1998). We present in this paper three new structures of the CheY–P2 complex obtained from two new crystal forms belonging to space group $P2_12_12_1$. Soaking experiments were performed on these crystals using acetyl phosphate, a phosphodonor, and imido-diphosphate, an inhibitor for the phosphorylation reaction. The native and derivatized structures were refined to 2.1, 2.4 and 2.7 Å resolution, respectively, and structural water molecules were included. Phosphorylated CheY was not trapped in phosphorylating conditions, but comparison of the native and the soaked crystals indicates significant changes in the active-site geometry. The binding of the inhibitor occurs in the immediate vicinity of the active site. Together, these results illustrate that the binding of CheY to P2 induces distant structural modifications that affect the active site of CheY and favours phosphorylation of the Asp57 residue.

2. Material and methods

2.1. Crystals

Crystallization of the CheY–CheA$_{124–257}$ complex in the presence of 10 m*M* manganese ions has been described previously (Welch *et al.*, 1998). Two new crystal forms were characterized in space group $P2_12_12_1$. Their unit-cell parameters are very similar: a = 157.6, b = 53.8, c = 76.6 Å for the first form and a = 159.3, b = 53.4, c = 77.8 Å for the second form. Each asymmetric unit contains two CheY–P2 complexes and 60% solvent. Before cryocooling in a stream of nitrogen gas at 100 K, crystals of the first form were transferred into a 2 µl droplet of the well solution containing 15% sucrose. Crystals of the second form were cryo-protected with 20% ethylene glycol. The data sets for the two orthorhombic crystal forms were not isomorphous. Plotting $\sum|F_{nat2} - F_{nat1}|/\sum F_{nat1}$ using *SCALEIT* from the *CCP*4 suite (Collaborative Computational Project, Number 4, 1994) gives an R_{iso} of 60% between the two native data sets; the structure determination confirms that the crystal packing in these two forms is different.

Table 1
Data collection and refinement statistics.

Values in parentheses are for the highest resolution shell (0.1 Å slice)

	Native	Acetyl phosphate	Imido-diphosphate
Data collection			
Unit-cell parameters (Å)	157.6, 53.8, 76.6	159.3, 53.4, 77.8	159.3, 53.4, 77.8
Resolution (Å)	30–2.1	30–2.4	30–2.7
Measured reflections	88506	63874	35121
Unique reflections	32997	26184	16044
Redundancy	2.7 (2.6)	2.4 (2.3)	2.2 (2.1)
Completeness (%)	85.2 (79.3)	96.5 (98.1)	85.9 (88.8)
$I/\sigma(I) > 3$ (%)	89.2 (77.7)	77.8 (47.9)	81.8 (54.2)
R_{sym} (%)	4.6 (15.1)	6.4 (20.0)	6.5 (19.1)
Refinement			
R (%)	18.8	21.7	21.3
R_{free} (%)	22.0	25.5	27.3
Resolution (Å)	15–2.1	15–2.4	15–2.7
R.m.s.d. bonds (Å)	0.014	0.014	0.009
R.m.s.d. angles (°)	1.6	1.5	1.3
Mean B factor (Å^2)	27	39	47
R.m.s.d. B, bonds (Å^2)			
Main-chain atoms	1.6	1.6	1.6
Side-chain atoms	2.6	2.7	2.3
R.m.s.d. B, angles (Å^2)			
Main-chain atoms	2.5	2.6	2.7
Side-chain atoms	3.9	3.8	3.5
No. of protein atoms	2982	2982	2982
No. of heteroatoms	264 H_2O, 2 Mn^{2+}	239 H_2O, 2 Mn^{2+}	165 H_2O, 2 Mn^{2+}, 1 imido-diphosphate

2.2. Structure determination

Native data from the first orthorhombic crystal form were collected to a resolution of 2.1 Å on beamline W32 (LURE, Orsay) on a 30 cm MAR Research image-plate detector. The crystal-to-detector distance was 290 mm, the oscillation range per image was 0.5° and the total oscillation angle was 94°. Images were processed with *DENZO* and *SCALEPACK* (Otwinowski & Minor, 1997) (Table 1). Phases were obtained by molecular replacement using *AMoRe* (Navaza, 1994) with the CheY and P2 molecules as search models (PDB code 1A0O). A solution was found with an R factor of 31% to 3.5 Å resolution. The structure was refined using *CNS* (Brunger *et al.*, 1998) and all data in the resolution range 15–2.1 Å. About 1500 reflections were kept apart for calculation of R_{free} values. Bulk-solvent correction and anisotropic temperature-factor scaling were applied and individual temperature factors were refined. Non-crystallographic symmetry (NCS) restraints between the two complexes were removed when the R factor reached 23%. The final refinement statistics are given in

Table 1. The structure of the P2 domain comprises residues 159–226. The flexible linkers at the N- and C-termini have no defined electron density. Each CheY–P2 complex binds a manganese ion in the active site of CheY as revealed by $F_o - F_c$ maps, which give peaks for the manganese ions at 16σ and 18σ above the mean density. The strongest peaks for water molecules were at 9σ. The average temperature factors are 25 and 30 Å^2 for CheY and P2, respectively.

Crystals of the second orthorhombic crystal form were soaked with acetyl phosphate or with imido-diphosphate at concentrations ranging from 10 to 200 m*M* before flash-cooling. The best diffraction patterns were obtained from crystals soaked either in 10 m*M* acetyl phosphate or 10 m*M* imido-diphosphate for 15 min (data collected to 2.4 and 2.7 Å resolution, respectively). Based on the crystal size and the unit-cell parameters, we evaluated the initial ratio between the number of molecules of acetyl phosphate *versus* the number of molecules of CheY to be about 50. Data processing was performed with *DENZO* and *SCALEPACK* (Otwinowski & Minor, 1997) (Table 1). These structures were solved by molecular replacement using the CheY and P2 molecules of the native orthorhombic form as search models. A solution was found with an *R*-factor value of 33% to 3.5 Å. The structure of the complex soaked with acetyl phosphate was refined to an *R* factor of 21.8% after removal of the NCS restraints. Inspection of the electron-density maps using *TURBO-FRODO* (Roussel & Cambillau, 1989) revealed no extra density corresponding to a phosphoryl group bound to Asp57. The structure of the complex soaked with imido-diphosphate was refined to an *R* factor of 22.6%. NCS restraints were maintained during crystallographic refinement. Only one molecule of imido-diphosphate was positioned in the asymmetric unit. CheY and P2 have average temperature factors of 34 and 45 Å^2, respectively, in the crystal soaked with acetyl phosphate, and 42 and 52 Å^2, respectively, in the crystal soaked with imido-diphosphate.

Sequence alignment was performed with *CLUSTAL* (Thompson *et al.*, 1994) and colour coded with *ESPript* (Gouet, Courcelle *et al.*, 1999). Secondary-structure elements and residue accessibility were calculated with *DSSP* (Kabsch & Sander, 1983). Structures were superposed using *LSQKAB* from the *CCP*4 suite (Collaborative Computational Project, Number 4, 1994). Hydrogen bonds were checked with *HBPLUS* (McDonald & Thornton, 1994). Figures were prepared with *MOLSCRIPT* (Kraulis, 1991).

3. Results

3.1. Overall structure and assembly

The six structures of CheY–P2 heterodimers determined from the asymmetric units of the native, the soaked acetyl phosphate and the soaked imido-diphosphate crystals are similar (r.m.s. deviations are 0.25 ± 0.05, 0.55 ± 0.05, 0.6 ± 0.1 Å for all C$^\alpha$ atoms of CheY, P2 and CheY–P2, respectively; Fig. 1). Only one large deviation arising from differences in the crystal packing environment is observed in the C$^\alpha$ trace of P2. It occurs at residues 201–203 of the loop β3–α2 and amounts to 2.6 Å for Asp202 (Fig. 1). Analysis of the crystal packing of the two orthorhombic crystal forms shows that the two heterodimers in each asymmetric unit are related by different NCS operators. The NCS rotation angle along the respective molecular axes is 20° in the first crystal form and 10° in the second form. The contacts between heterodimers in both crystal forms nevertheless involve an homologous CheY–CheY interface (300 Å^2), which prevents access to the active site of CheY in one CheY–P2 complex in each asymmetric unit (Fig. 1). In the other CheY–P2 complexes in the asymmetric units, the active site of CheY is fully exposed to the solvent and is accessible to substrate *via* water channels 20–30 Å in diameter. A second common feature of the two crystal forms is that the β-sheets of symmetry-related P2 domains are in contact *via* a conserved interface, which excludes 900 Å^2 from solvent. This suggests a possible site of dimerization for CheY–P2 complexes through the P2 domain (Welch *et al.*, 1998). Interestingly, the measured correlation time for this complex from time-resolved fluorescence studies indicates that the CheY–P2 complex exists as dimers in solution (F. Mérola, J. Stock, P. Gouet & J.-P. Samama, unpublished data).

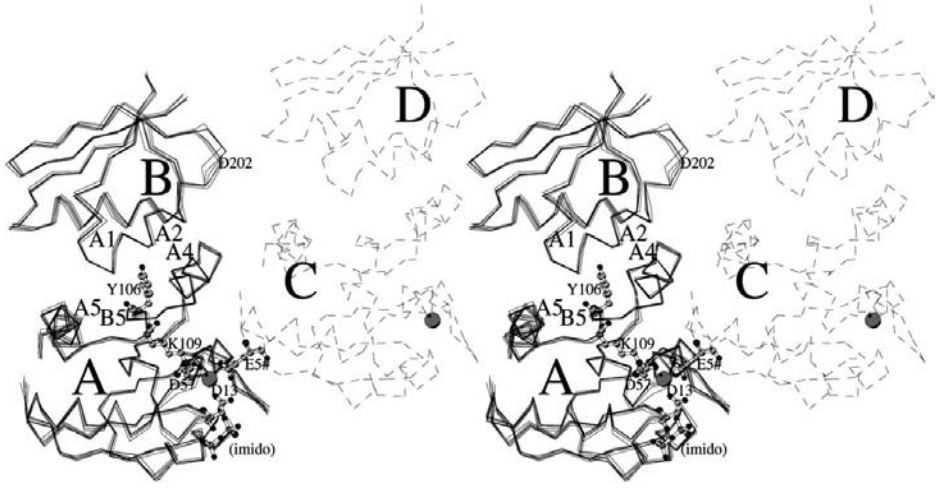

Figure 1
Stereoview of the two CheY–P2 heterodimers, *A*–*B* and *C*–*D*, contained in the asymmetric unit. The C$^\alpha$ traces of the three *A*–*B* complexes (native, soaked acetyl phosphate, soaked imido-diphosphate) are superposed in plain lines. The *C*–*D* heterodimer of the native is shown as a dotted line. The bound manganese is shown as a grey sphere. The important residues Asp13, Asp57, Tyr106 and Lys109 are drawn as sticks for the *A* monomer. Glu5 of monomer C which points toward the active site of molecule *A* is presented. The binding site of imido-diphosphate is also shown near the first α-helix.

3.2. The CheY–P2 heterodimer

CheY and P2 molecules associate through a conserved interface which buries a surface area of 1200 Å^2. The heterodimer interface involves the C-terminal face of CheY, α4–β5–α5, and the α1 and α2 helices of P2 (Figs. 1 and 2). Complex formation induces limited structural changes in the receiver domain. P2-bound and isolated CheYs (Volz & Matsumura, 1991) can be superposed with an r.m.s. deviation of 0.5 Å. The largest deviations (0.8–1.6 Å) are observed for residues 87–94 in the β4–α4 loop, which is close to the protein–protein interface. In contrast, a significant shift of the two helices of the P2 domain is observed when comparing the NMR structure of isolated P2 (McEvoy *et al.*, 1996) to that of the CheY-bound P2 domain. The r.m.s.d. is 1.8 Å for all C$^\alpha$ pairs, suggesting that the CheY–P2 interactions are optimized through rigid-body movements in the P2 domain.

The same residues contribute to the protein–protein interface in all crystal forms (Welch *et al.*, 1998; McEvoy *et al.*, 1998; this work). The network of interactions is identical in all CheY–P2 complexes solved in this study and the surface complementarity (Lawrence & Colman, 1993) at the interface region is excellent, Sc = 0.74. The five water molecules bridging residues of CheY to residues of P2 in the high-resolution native structure (Fig. 3) are also found in the CheY–P2 complexes soaked with acetyl phosphate and with imidodiphosphate. One of these water molecules is hydrogen bonded to the phenol group of the functionally important Tyr106 (Zhu *et al.*, 1996, 1997). Tyr106 was observed as a two-state conformer in isolated CheY (Volz & Matsumura, 1991), with one rotamer inside and the other outside the protein core. The second rotamer is selected in the CheY–P2 complex, where the phenol group interacts with residues Glu178 and His181 from the P2 domain (Fig. 3).

3.3. The active site

The binding of a metal ion in the active site of CheY in all CheY–P2 heterodimers is unambiguous with regards to the electron density (see §2). In the native structure, the cation is liganded by one O atom from the carboxylate groups of Asp13 and Asp57, by the main-chain carbonyl O atom of Asn59 and by a single water molecule. Two sites of the octahedral coordination sphere of the metal cation are empty (Fig. 4*a*). The ε-amino group of Lys109 is hydrogen bonded to Asp12 through a water molecule and forms a salt-bridge interaction with Asp57 (2.8 Å). In the other CheY–P2 complex in the asymmetric unit, the active site of CheY is shielded by crystal packing interactions. The carboxylate group of Glu5 from a NCS-related CheY molecule is at a hydrogen-bond distance from Lys109 and the Mn^{2+} ion (Fig. 4*b*). This geometry may mimic the approach of the phosphohistidine to the active site of response regulators and was also observed in the CheY–P2 structure reported by McEvoy *et al.* (1998).

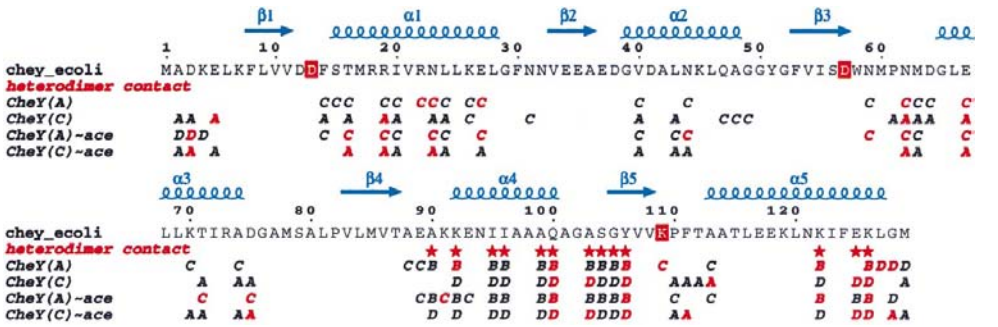

Figure 2
Sequence and secondary-structure elements of *E. coli* CheY in the complex. Helices and β-strands are shown in blue as squiggles and arrows. The three residues invariant in all receiver domains are boxed in red. Residues of CheY (molecules *A* and *C*) involved in intermolecular contacts are represented below the sequence. The letter of the contacting molecule (*A*, *B*, *C* or *D*) is written in red if there is at least one atom located at less than 3.2 Å and in black for 3.2–4 Å contacts. Red stars denote residues located at the CheY–P2 interface.

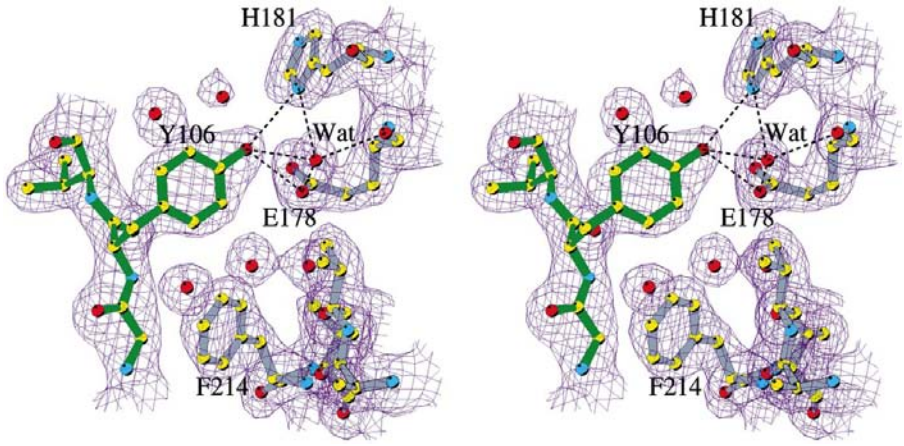

Figure 3
Close-up view at the heterodimer interface illustrating the environment of Tyr106 in CheY and of Glu178, His181 and Phe214 in P2. The $2F_o - F_c$ map of the 2.1 Å resolution native structure is contoured at 1σ.

3.4. The soaked compounds

CheY has a significant autophosphatase activity, expressed by a half-life of about 20 s for phospho-CheY (Lukat *et al.*, 1992), that impairs the structure determination by crystallographic methods. Our soaking experiments with acetyl phosphate aimed to detect possible structural traces of a

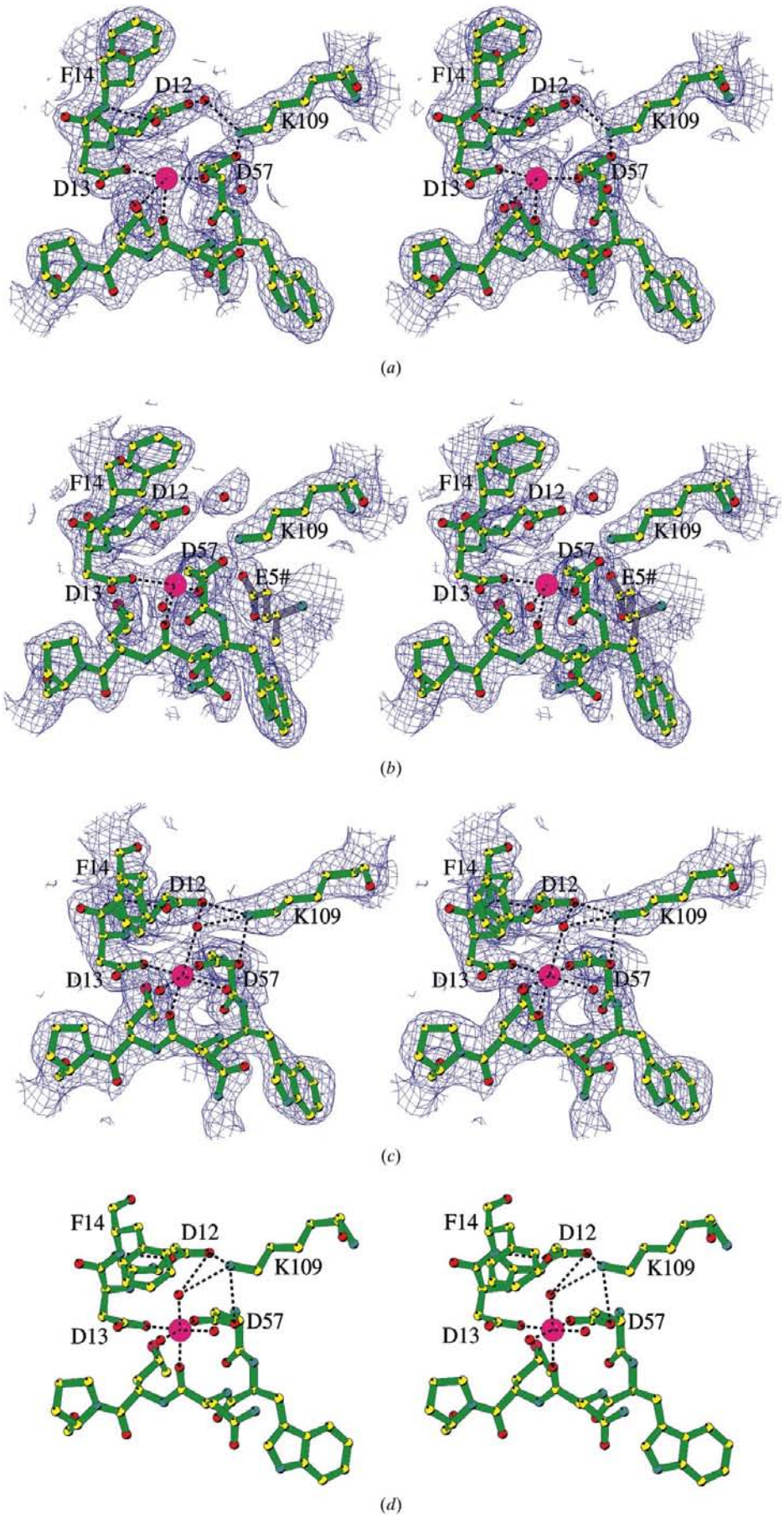

phosphorylation–dephosphorylation process. This process was expected to be completed in the crystal after 15 min, according to the fast kinetics of the reaction (Da Re *et al.*, 1999) and to the molar ratio of phosphodonor to CheY in the crystal (see §2). CheY–P2 crystals that experienced soaking with acetyl phosphate display significant differences in the active site of CheY exposed to solvent and accessible to the phosphodonor (Fig. 4*c*). The carboxylate group of the phosphoacceptor Asp57 has rotated by an angle $\Delta\chi_2$ of 20°. One of its Oδ atoms is at a distance of 3.0 Å from the ε-amino group of the conserved Lys109, which is also hydrogen bonded to Asp12. The manganese ion now displays a full octahedral coordination. The side chain of Phe14 is displaced from the upward position found in the native structure, which increases the accessibility to Asp57, to a downward position ($\Delta\chi_1$ = 95°; Fig. 4*c*). This geometry is extremely similar to that found in Mg^{2+}-bound isolated CheY (Fig. 4*d*) (Bellsolell *et al.*, 1994).

One molecule of imido-diphosphate was modelled in the structure of the complex soaked with this inhibitor (Fig. 5). Imido-diphosphate belongs to a group of phosphoorganic compounds identified by Aventis scientists as weak inhibitors of phosphorylation of the response regulator by acetyl phosphate and histidine kinases (A. Denis, personal communication). The inhibitor is fully visible in the electron-density maps computed at 2.7 Å resolution. It binds in the vicinity of residues 13–15 of CheY, at a van der Waals

Figure 4
Close-up view of the CheY active site and of the arrangement of water molecules (small pink spheres) around the bound manganese ion (large pink sphere) and the $2F_o - F_c$ maps (1σ). (*a*) The solvent-accessible active site in the native structure; (*b*) the active site shielded by Glu5 from a symmetry-related molecule; (*c*) the solvent-accessible active site in the complex soaked with acetyl phosphate; (*d*) the active site in isolated CheY (Bellsolell *et al.*, 1994).

distance to the phenyl ring of Phe14. One phosphate moiety is hydrogen-bonded to the main-chain N atom and the hydroxyl group of Ser15. The other part of the inhibitor makes interactions with the main-chain carbonyl of the conserved Asp13 and is bridged to the carboxylate of this residue *via* a water molecule.

4. Discussion

Our structural results indicate that the specificity of the binding of CheY to $CheA_{159–226}$ (the P2 domain) is driven by the remarkable complementarity of the interface region which generates a locked heterodimer. Its conservation in detail in all our crystal forms contrasts with the flexibility reported for the same complex obtained from a slightly different construct of the P2 domain and crystallized under different conditions and in the absence of bound metal ion (McEvoy *et al.*, 1998). The specificity of the molecular recognition is essential *in vivo* to avoid activation by CheA of the several other response regulators dedicated to different metabolic or behavioural cell responses (Mizuno, 1998). Formation of the CheY–CheA complex may also be a means of increasing the local concentration of the substrate (CheY) for a more efficient activation by phospho-$CheA_{1–134}$ (the P1 domain).

The association between the kinase and the response regulator is disrupted by subtle changes at the interface region (Bischoff *et al.*, 1993). In the signalling process, these changes occur upon phosphorylation of CheY, which causes a sixfold increase in the K_d value (2 μM) for the complex (Li *et al.*, 1995) and leads to the release of phospho-CheY. The detailed features of these conformational changes were revealed by the recent X-ray structure determinations of the phosphorylated homologous receiver domains Spo0A (Lewis *et al.*, 1999) and FixJN (Birck *et al.*, 1999). In both phosphorylated domains the conserved aromatic side chain at the equivalent position to Tyr106 adopts a buried position within the protein core. This orientation was also observed in the NMR structure of BeF_3-activated CheY (Cho *et al.*, 2000) and in the X-ray structure of phospho-CheY, an activated analogue of CheY (Halkides *et al.*, 2000). The displacement of the aromatic side chain from the solvent-exposed position in unphosphorylated species to the inside position in phosphorylated receiver domains is clearly a post-phosphorylation event and is an important factor in the signalling property of the response regulator (Zhu *et al.*, 1996). It concludes a cascade of conformational changes that alters the $\alpha4$–$\beta5$–$\alpha5$ surface of the receiver domains to different extents (Birck *et al.*, 1999; Kern *et al.*, 1999; Lewis *et al.*, 1999; Cho *et al.*, 2000; Halkides *et al.*, 2000). This remodelling of the signalling surface is a general feature in two-component systems that disrupts previous interactions mediated by the receiver domain and fosters new ones, such as dimerization of phospho-FixJ (Birck *et al.*, 1999). In the case of CheY, it directly affects the CheY–P2 interface and explains the dissociation of the complex upon phosphorylation in solution.

The 2.4 Å resolution structure of the CheY–P2 complex soaked with acetyl phosphate displays none of the phosphorylation-induced structural effects. The question arises whether the CheY protein has experienced a phosphorylation–dephosphorylation process within the crystalline complex. The differences observed in the active site of the solvent-accessible CheY before and after soaking with acetyl phosphate suggest that this process has occurred. The active site of CheY in the native CheY-P2 structure is readily accessible through the upward position of Phe14. It offers two empty coordination sites for the manganese ion and therefore presents the features expected for the formation of the transition state in the phosphotransfer reaction (Stock *et al.*, 1993). These coordination sites may be filled by two O atoms of the incoming phosphoryl group, leading to the bipyramidal transition state that favours the in-line attack of the P atom by Asp57. Dephosphorylation is known to occur readily in CheY since the half-life of the acyl-phosphate group is only 20 s. According to the structure of the complex after soaking with acetyl phosphate, the active site of CheY appears to be in a 'resting state' in which the accessibility is restricted by the downward position of Phe14 and where all coordination sites of the metal ion are occupied by water molecules. To date, no difference has been reported between Mn^{2+}- or Mg^{2+}-bound structures of receiver domains (Usher *et al.*, 1998; Gouet, Fabry *et al.*, 1999) and our observations must be valid for an Mg^{2+}-bound complex.

It might be argued that the impaired movement of Tyr106 within the crystalline CheY–P2 complex may prevent phosphorylation of CheY by acetyl phosphate. However, as already mentioned, the displacement of Tyr106 is a post-phosphorylation event and is only essential for the signalling properties of the response regulator. This was illustrated by the study of CheY proteins bearing the T87I mutation. The T87I and T87I/Y106W CheY mutants are

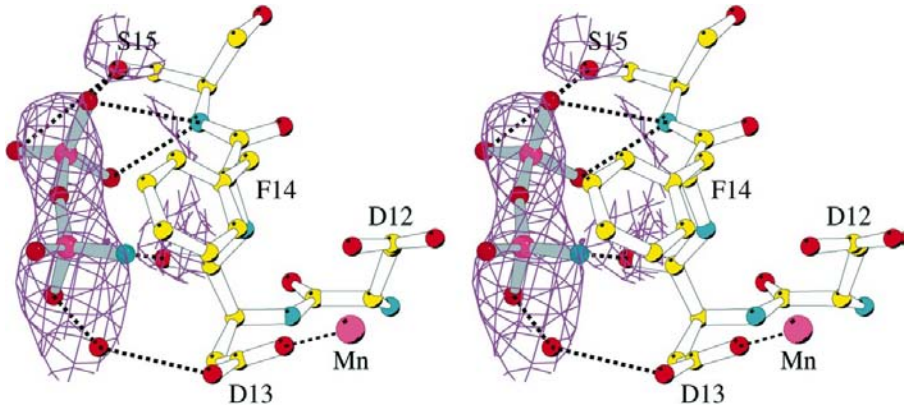

Figure 5
Stereoview of the bound imido-diphosphate and its network of electrostatic interactions. The 2.7 Å $2F_o - F_c$ map is contoured at 1σ.

phosphorylatable *in vitro* (Zhu *et al.*, 1997) but are non-chemotactic. This is because they cannot undergo conformational changes upon phosphorylation since Ile87 sterically prevents the aromatic side chain of Tyr106 or Trp106 from rotating inside the protein core (Zhu *et al.*, 1996, 1997). These results and our study are complementary in the sense that both observations show that constraining the hydrophobic side chain of residue 106 in the external rotameric position uncouples phosphorylation and conformational change of CheY. In our experiment, the rotameric conformation of the Tyr106 side chain is stabilized by hydrogen bonds to the P2 domain in a crystalline complex stabilized by packing forces that evidently prevent dissociation of CheY and P2 upon phosphorylation of CheY. The free energy associated with the crystal packing forces apparently counteracts the variation of free energy between unphosphorylated and phosphorylated CheY. Interestingly, we observed that the diffraction pattern (mosaicity and diffraction limit) of the CheY–P2 crystals was severely affected in a reproducible way when acetyl phosphate was still available in the soaking medium (after 5 and 10 min) and only improved after full consumption of the phosphorylating agent. These disturbances of the crystal lattice are likely to reflect the expected conformational fluctuations in the course of the phosphorylation–dephosphorylation process.

In several instances, molecular communication between the active site and remote regions in receiver domains has been reported, in line with the ability of receiver domains to propagate structural changes from the signalling surface to the 20 Å distant active site (Lowry *et al.*, 1994; Halkides *et al.*, 2000). The downward conformation of the Phe14 side chain observed in isolated wild-type CheY (Volz & Matsumura, 1991) shifts to the upward conformation, which increases the accessibility of the active site in the native CheY–P2 complex (Welch *et al.*, 1998; McEvoy *et al.*, 1998), in the hypertumbling Y106W mutant of CheY (Zhu *et al.*, 1997), in the BeF_3-activated CheY (Cho *et al.*, 2000) and in CheY in complex with the HPt domain of ArcB (Kato *et al.*, 1999). Phe14 belongs to the $\beta1$–$\alpha1$ loop, shown by NMR studies of Spo0F (Feher & Cavanagh, 1999) and X-ray crystallography of FixJN (Gouet, Fabry *et al.*, 1999) to display significant flexibility and to shift position upon phosphorylation (Birck *et al.*, 1999). Imidodiphosphate interacts with residues 13–15. The inhibitory effect of this compound on phosphorylation may therefore arise from tightening the conformation of this region. This emphasizes the importance of the dynamic properties of this region in the catalytic processes and also in the recognition of protein partners as illustrated in the Spo0F–Spo0B complex (Zapf *et al.*, 2000).

References

Baikalov, I., Schroder, I., Kaczor-Grzeskowiak, M., Grzeskowiak, K., Gunsalus, R. P. & Dickerson, R. E. (1996). *Biochemistry*, **35**, 11053–11061.

Barak, R. & Eisenbach, M. (1996). *Curr. Top. Cell Regul.* **34**, 137–158.

Bellsolell, L., Prieto, J., Serrano, L. & Coll, M. (1994). *J. Mol. Biol.* **238**, 489–495.

Bilwes, A. M., Alex, L. A., Crane, B. R. & Simon, M. I. (1999). *Cell*, **96**, 131–141.

Birck, C., Mourey, L., Gouet, P., Fabry, B., Schumacher, J., Rousseau, P., Kahn, D. & Samama, J.-P. (1999). *Structure*, **7**, 1505–1515.

Bischoff, D. S., Bourret, R. B., Kirsch, M. L. & Ordal, G. W. (1993). *Biochemistry*, **32**, 9256–9261.

Bren, A. & Eisenbach, M. (1998). *J. Mol. Biol.* **278**, 507–514.

Brunger, A. T., Adams, P. D., Clore, G. M., DeLano, W. L., Gros, P., Grosse-Kunstleve, R. W., Jiang, J. S., Kuszewski, J., Nilges, M., Pannu, N. S., Read, R. J., Rice, L. M., Simonson, T. & Warren, G. L. (1998). *Acta Cryst.* D**54**, 905–921.

Cho, H. S., Lee, S. Y., Yan, D., Pan, X., Parkinson, J. S., Kustu, S., Wemmer, D. E. & Pelton, J. G. (2000). *J. Mol. Biol.* **297**, 543–551.

Collaborative Computational Project, Number 4 (1994). *Acta Cryst.* D**50**, 760–763.

Da Re, S., Deville-Bonne, D., Tolstykh, T., Véron, M. & Stock, J. B. (1999). *FEBS Lett.* **457**, 323–326.

Dutta, R., Qin, L. & Inouye, M. (1999). *Mol. Microbiol.* **34**, 633–640.

Feher, V. A. & Cavanagh, J. (1999). *Nature (London)*, **400**, 289–293.

Goudreau, P. N. & Stock, A. M. (1998). *Curr. Opin. Microbiol.* **1**, 160–169.

Gouet, P., Courcelle, E., Stuart, D. I. & Metoz, F. (1999). *Bioinformatics*, **15**, 305–308.

Gouet, P., Fabry, B., Guillet, V., Birck, C., Mourey, L., Kahn, D. & Samama, J.-P. (1999). *Structure*, **7**, 1517–1526.

Grebe, T. W. & Stock, J. B. (1999). *Adv. Microb. Physiol.* **41**, 139–227.

Halkides, C. J., McEvoy, M. M., Casper, E., Matsumura, P., Volz, K. & Dahlquist, F. W. (2000). *Biochemistry*, **39**, 5280–5286.

Kabsch, W. & Sander, C. (1983). *Biopolymers*, **22**, 2577–2637.

Kato, M., Shimizu, T., Mizuno, T. & Hakoshima, T. (1999). *Acta Cryst.* D**55**, 1257–1263.

Kern, D., Volkman, B. F., Luginbuhl, P., Nohaile, M. J., Kustu, S. & Wemmer, D. E. (1999). *Nature (London)*, **402**, 894–898.

Kraulis, P. J. (1991). *J. Appl. Cryst.* **24**, 946–950.

Lawrence, M. C. & Colman, P. M. (1993). *J. Mol. Biol.* **234**, 946–950.

Levit, M. N., Liu, Y. & Stock, J. B. (1998). *Mol. Microbiol.* **30**, 459–466.

Lewis, R. J., Brannigan, J. A., Muchova, K., Barak, I. & Wilkinson, A. J. (1999). *J. Mol. Biol.* **294**, 9–15.

Li, J., Swanson, R. V., Simon, M. I. & Weis, R. M. (1995). *Biochemistry*, **34**, 14626–14636.

Liu, Y., Levit, M., Lurz, R., Surette, M. G. & Stock, J. B. (1997). *EMBO J.* **16**, 7231–7240.

Lowry, D. F., Roth, A. F., Rupert, P. B., Dahlquist, F. W., Moy, F. J., Domaille, P. J. & Matsumura, P. (1994). *J. Biol. Chem.* **269**, 26358–26362.

Lukat, G. S., McCleary, W. R., Stock, A. M. & Stock, J. B. (1992). *Proc. Natl Acad. Sci. USA*, **89**, 718–722.

McDonald, I. K. & Thornton, J. M. (1994). *J. Mol. Biol.* **238**, 777–793.

McEvoy, M. M., Bren, A., Eisenbach, M. & Dahlquist, F. W. (1999). *J. Mol. Biol.* **289,** 1423–1433.

McEvoy, M. M., Hausrath, A. C., Randolph, G. B., Remington, S. J. & Dahlquist, F. W. (1998). *Proc. Natl Acad. Sci. USA*, **95**, 7333–7338.

McEvoy, M. M., Muhandiram, D. R., Kay, L. E. & Dahlquist, F. W. (1996). *Biochemistry*, **35**, 5633–5640.

Madhusudan, Zapf, J., Hoch, J. A., Whiteley, J. M., Xuong, N. H. & Varughese, K. I. (1997). *Biochemistry*, **36**, 12739–12745.

Mizuno, T. (1998). *J. Biochem.* **123**, 555–563.

Müller-Dieckmann, H.-J, Grantz, A. A. & Kim, S.-H. (1999). *Structure*, **7**, 1547–1556.

Navaza, J. (1994). *Acta Cryst.* A**50**, 157–163.

Oosawa, K., Hess, J. F. & Simon, M. I. (1988). *Cell*, **53**, 89–96.

Otwinowski, Z. O. & Minor, W. (1997). *Methods Enzymol.* **276**, 307–326.

Roussel, A. & Cambillau, C. (1989). *Silicon Graphics Geometry Partner Directory*, edited by Silicon Graphics, pp. 77–78. Silicon Graphics, Mountain View, CA, USA.

Sola, M., Gomis-Ruth, F., Serrano, L., Gonzalez, A. & Coll, M. (1999). *J. Mol. Biol.* **285**, 675–687.

Stock, A. M., Martinez-Hackert, E., Rasmussen, B. F., West, A. H., Stock, J. B., Ringe, D. & Petsko, G. A. (1993). *Biochemistry*, **32**, 13375–13380.
Stock, A. M., Mottonen, J. M., Stock, J. B. & Schutt, C. E. (1989). *Nature (London)*, **337**, 745–749.
Stock, J. B., Surette, M. G., Levit, M. & Park, P. (1995). *Two-Component Signal Transduction*, edited by J. A. Hoch & T. Silhavy, pp. 25–51. Washington, DC: American Society of Microbiology.
Swanson, R. V., Lowry, D. F., Matsumura, P., McEvoy, M. M., Simon, M. I. & Dahlquist, F. W. (1995). *Nature Struct. Biol.* **2**, 906–910.
Thompson, J. D., Higgins, D. G. & Gibson, T. J. (1994). *Nucleic Acids Res.* **22**, 4673–4680.
Usher, K. C., Cruz, A. F., Dahlquist, F. W., Swanson, R. V., Simon, M. I. & Remington, S. J. (1998). *Protein Sci.* **7**, 403–412.
Volkman, B. F., Nohaile, M. J., Amy, N. K., Kustu, S. & Wemmer, D. E. (1995). *Biochemistry*, **34**, 1413–1424.
Volz, K. & Matsumura, P. (1991). *J. Biol. Chem.* **266**, 15511–15519.
Welch, M., Chinardet, N., Mourey, L., Birck, C. & Samama, J. P. (1998). *Nature Struct. Biol.* **5**, 25–29.
Zapf, J., Sen, U., Madhusudan, Hoch, J. A. & Varughese, K. I. (2000) *Structure Fold. Des.* **8**, 851–862.
Zhou, H., Lowry, D. F., Swanson, R. V., Simon, M. I. & Dahlquist, F. W. (1995). *Biochemistry*, **34**, 13858–13870.
Zhu, X., Amsler, C. D., Volz, K. & Matsumura, P. (1996). *J. Bacteriol.* **178**, 4208–4215.
Zhu, X., Rebello, J., Matsumura, P. & Volz, K. (1997). *J. Biol. Chem.* **272**, 5000–5006.